

Article

Biochemical Characterization of the SPATE Members EspP α and EspI

André Weiss, David Kortemeier and Jens Brockmeyer *

Institute of Food Chemistry, Corrensstraße 45, 48149 Münster, Germany

* Author to whom correspondence should be addressed; E-Mail: jbrockm@uni-muenster.de;
Tel.: +49-251-83-33392; Fax: +49-251-83-33396.

Received: 3 July 2014; in revised form: 18 August 2014 / Accepted: 21 August 2014 /

Published: 16 September 2014

Abstract: The activity of serine proteases is influenced by their substrate specificity as well as by the physicochemical conditions. Here, we present the characterization of key biochemical features of the two SPATE members EspP α and EspI from Shiga-toxin producing *Escherichia coli* (STEC) and enterohemorrhagic *E. coli* (EHEC). Both proteases show high activity at conditions mimicking the human blood stream. Optimal activities were observed at slightly alkaline pH and low millimolar concentrations of the divalent cations Ca²⁺ and Mg²⁺ at physiological temperatures indicating a function in the human host. Furthermore, we provide the first cleavage profile for EspI demonstrating pronounced specificity of this protease.

Keywords: EspP α ; EspI; SPATE; virulence factor; EHEC; STEC; biochemical characterisation; substrate specificity

1. Introduction

The serine protease autotransporters of *Enterobacteriaceae* (SPATE) are a family of virulence factors, which are transported via the type V or classical autotransporter pathway. SPATEs harbor a serine protease motif inside their passenger domain and it is believed that SPATE proteins mediate their virulence—at least partially—via proteolytic cleavage of host proteins. The plasmid-encoded extracellular serine protease EspP belongs to the SPATE family and is present in the supernatant of Shiga-toxin producing *Escherichia coli* (STEC) and enterohemorrhagic *E. coli* (EHEC) [1,2]. Five subtypes of EspP have been described (EspP α -EspP ϵ) [3,4] from which EspP α is clearly associated

with highly pathogenic EHEC serotypes and with isolates from patients with severe disease [3,5]. EspP α has been shown to cleave porcine pepsin A, coagulation factor V, apolipoprotein A-I, the complement factors C3 and C5, and EHEC-hemolysin [1,6–8]. *E. coli* secreted protease, island-encoded (EspI) is a further member of the SPATE family and is found, like EspP, in Shiga-toxin producing *E. coli* [6]. Notably, this SPATE is associated with less pathogenic STEC [6,9–11]. It has been shown that EspI, like EspP α , cleaves porcine pepsin A and apolipoprotein A-I [6]. The physiological function of EspI remains to be elucidated.

EspI has not been characterized systematically on functional level and studies concerning functionality of EspP α have focused mainly on potential implications of this virulence factor in terms of pathogenicity of EHEC infection [1–3,7,8,12–14]. The activity of serine proteases is influenced besides the inherent substrate specificity by physicochemical aspects, such as temperature, pH, and composition of the solvent [15]. Studies addressing these biochemical aspects of EspP α and EspI are still lacking. Therefore, we present here the determination of temperature and pH-optima and the influence of divalent ions such as Mg²⁺ or Ca²⁺ on proteolytic activity, which allows to estimate to a certain extent for which environmental conditions the respective enzymes might be optimized. Furthermore, we present a cleavage profile of EspI using short chromogenic peptides as substrates to elucidate specificity of this protease.

2. Results and Discussion

2.1. Purification of EspP α and EspI

EspP α and EspI were purified from culture supernatants using ammonium sulfate precipitation and liquid chromatography. Purity was verified via SDS-PAGE (Figure 1) and the identity of autoproteolysis bands was verified by MALDI-TOF-MS (data not shown). As expected, EspP α samples showed a pronounced protein band at ~104 kDa representing the intact EspP α . Another band at ~80 kDa was identified as an autoproteolysis product of EspP α . The protein pattern of the EspI sample showed a protein band at ~110 kDa (intact EspI), as well as two autoproteolysis products of EspI at ~60 and 50 kDa, respectively. Autoproteolysis products of both proteases are still active even after long term incubation (data not shown).

2.2. Temperature Optimum of EspP α and EspI

The influence of the incubation temperature on the activity of EspP α and EspI was investigated using the chromogenic oligopeptide substrate succinic acid-alanine-alanine-proline-leucine-(para-nitroaniline) (Suc-Ala-Ala-Pro-Leu-pNA) in a temperature profile ranging from 20 °C to 55 °C for EspP α and 10 °C to 60 °C for EspI, respectively. For EspP α , maximum relative activity was observed at ~40 °C (T_{opt}) and 50% activity values at ~26 °C and ~45 °C, respectively (Figure 2a). Activity decreased rapidly when temperature exceeded T_{opt} and complete loss of activity was observed at 50 °C (Figure 2a). In order to investigate if rapid loss of activity at increased temperatures is due to irreversible heat denaturation or reversible misfolding, EspP α was pre-incubated for 30 min at temperatures ranging from 50 °C to 70 °C followed by determination of residual activity at 37 °C (Figure 2b). No loss of activity was observed after pre-incubation at 50 °C, indicating that decreasing activity of EspP α in the

temperature range from 40 to 50 °C is due to reversible structural alterations of EspPα. This assumption was further supported by the observation that also prolonged pre-incubation at 50 °C up to 240 min only slightly affected the residual activity of EspPα (data not shown). Increasing heat denaturation occurred at temperatures exceeding 50 °C with complete loss of activity after 30 min of pre-incubation at 60 °C or higher temperatures (Figure 2b).

Figure 1. Purification of EspPα and EspI (**left**) SDS-PAGE of purified EspPα. *, EspPα autoproteolysis product; (**right**) SDS-PAGE of purified EspI. *, EspI autoproteolysis product. M = Molecular weight marker. Purity (including autoproteolysis products) of both samples was >95% as determined by densitometrical analysis of SDS-PAGE gels.

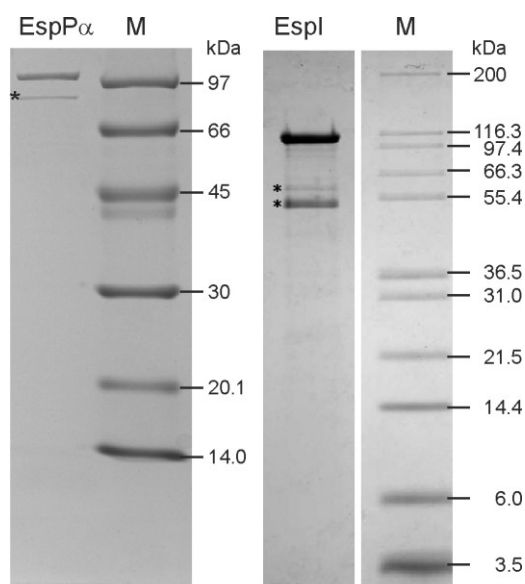
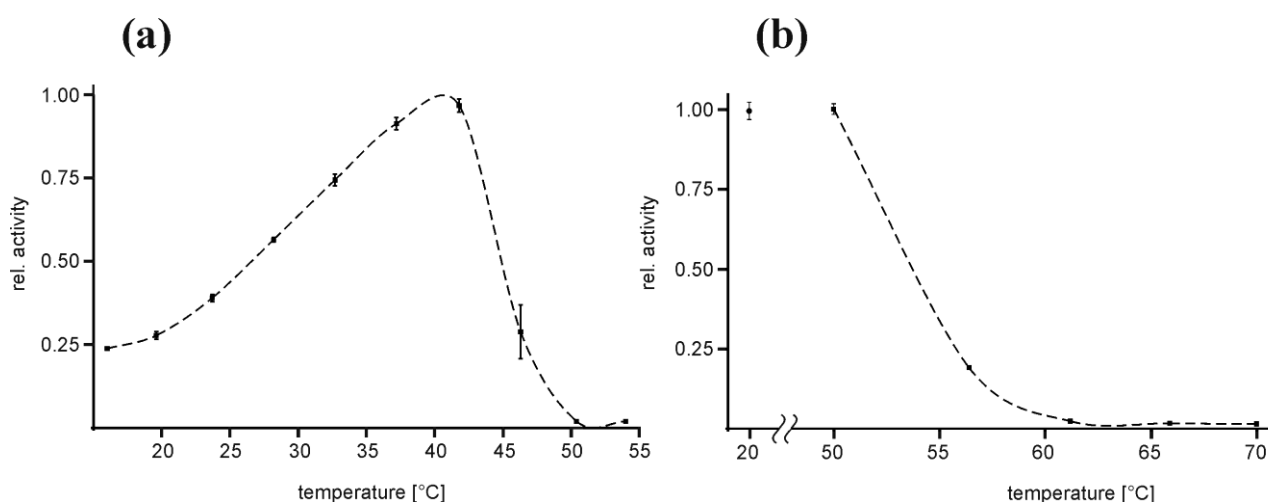
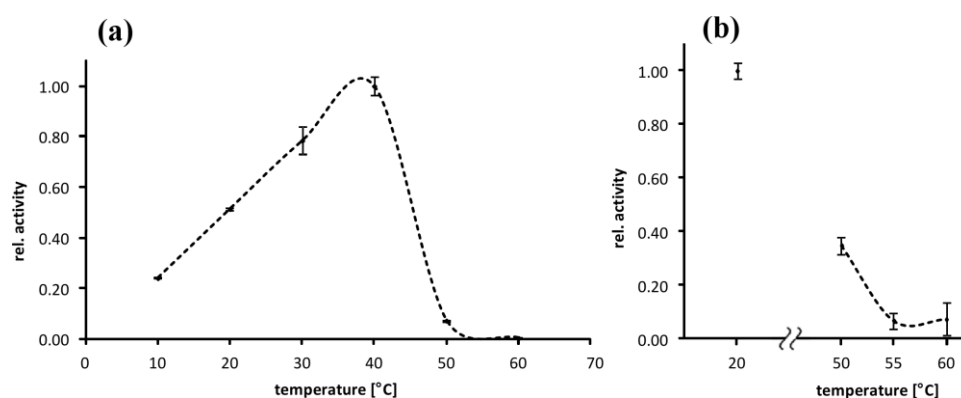


Figure 2. Temperature optimum and heat denaturation of EspPα (**a**) Relative activity of EspPα at varying incubation temperatures. Relative activity is normalized to T_{opt} at ~40 °C, $n = 8$; (**b**) Effect of 30 min pre-incubation at elevated temperatures on the activity of EspPα at 37 °C. Pre-incubation temperatures are given in the x -axis and the relative activity was subsequently determined at 37 °C. The negative control was incubated for 30 min at 20 °C. Relative activity is normalized to the negative control, $n = 8$.



The temperature dependence of EspI-activity is similar to EspP α . Maximum relative activity of EspI was observed at ~ 38 °C (T_{opt}) and 50% values at ~ 20 °C and ~ 45 °C, respectively (Figure 2a). EspI activity increased linearly from 10 °C to T_{opt} and further temperature increase resulted in rapid reduction of EspI activity with complete loss of activity at ~ 50 °C (Figure 3a). In contrast to EspP α , pre-incubation at 50 °C lead to significant loss of activity (residual activity < 40%) indicating EspI is more prone to heat denaturation than EspP α . Pre-incubation at 55 °C and 60 °C leads to almost complete loss of activity (Figure 3b).

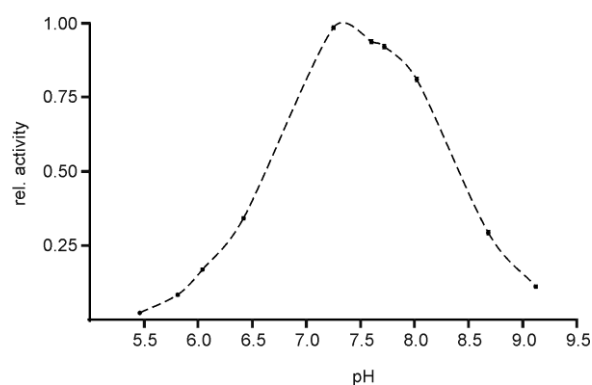
Figure 3. Temperature optimum and heat denaturation of EspI (a) Relative activity of EspI at varying incubation temperatures. Relative activity is normalized to T_{opt} at ~ 38 °C, $n = 3$; (b) Effect of 120 min pre-incubation at elevated temperatures on the activity of EspI at 37 °C. Pre-incubation temperatures are given in the x-axis and the relative activity was subsequently determined at 37 °C. The negative control was incubated for 120 min at 20 °C. Relative activity is normalized to the negative control, $n = 3$.



2.3. pH Optimum of EspP α and EspI

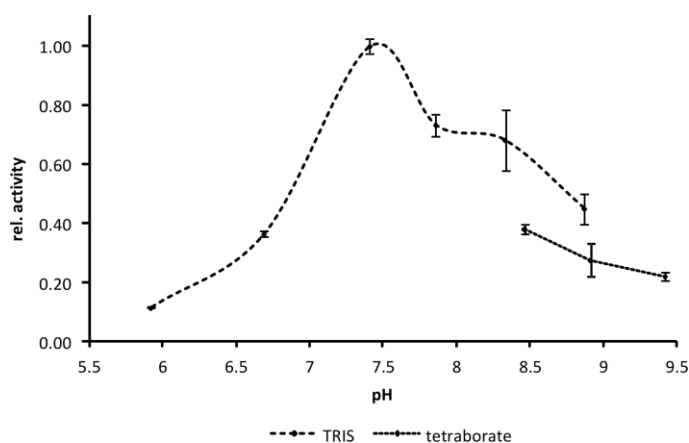
Determination of pH dependence of EspP α activity revealed a pronounced optimum at pH values of ~ 7.5 and relative activity of 50% at pH 6.6 and 8.4 (Figure 4). Buffer conditions with pH values below 6.0 or above 9.0 resulted in nearly complete loss of proteolytic activity of EspP α , indicating that this protease is highly optimized for environmental conditions in a slightly alkaline milieu between pH 7 and 8.

Figure 4. Determination of the pH optimum of EspP α . Activity of EspP α was determined in the pH range from 5.5 to 9.1. The proteolytic activity is expressed relative to pH_{opt} at ~ 7.4 , $n = 5$.



EspI activity shows a pronounced maximum at pH ~ 7.5 and relative activity of 50% at pH 6.8 and 8.7. Decreasing pH values lead to rapid loss of activity while more alkaline conditions led to only slow reduction of activity (Figure 5).

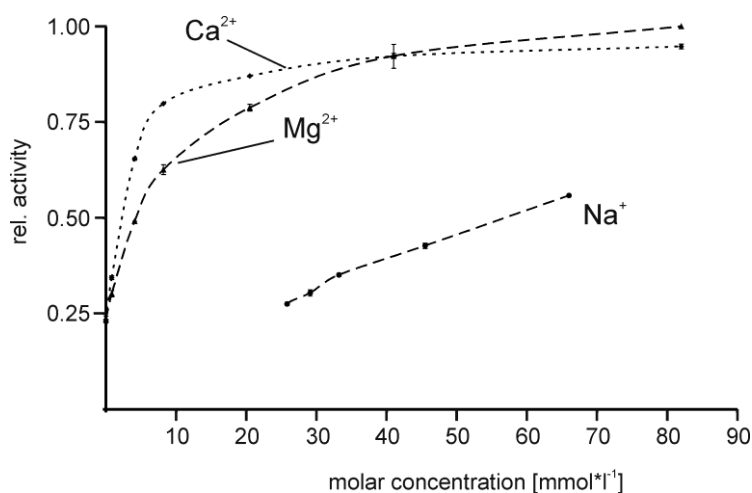
Figure 5. Determination of the pH optimum of EspI. Activity of EspI was determined in the pH range from 5.9 to 9.4. The proteolytic activity is expressed relative to pH_{opt} at ~ 7.5 . Note that EspI activity in TRIS buffer is higher than in tetraborate buffer. $n = 4$.



2.4. Effect of Buffer Composition

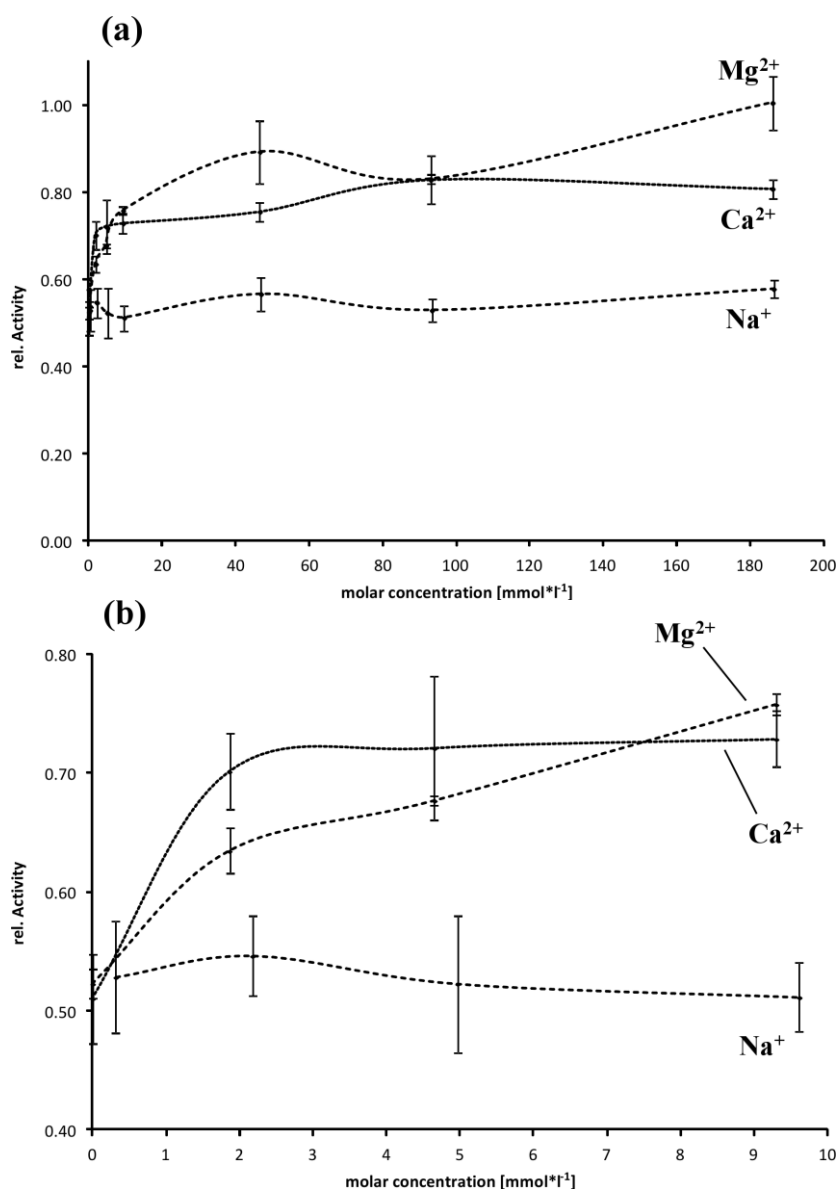
The addition of divalent cations significantly affected proteolytic activity of EspP α . Supplementation with up to 8 mM CaCl₂ resulted in nearly fourfold increased activity of EspP α in a dose-dependent manner when compared to the respective buffer lacking divalent cations. Further increase of the Ca²⁺ concentration resulted in plateau formation of EspP α activity, suggesting saturation with Ca²⁺ (Figure 6). The addition of MgCl₂ led to similar effects though the activity plateau was reached at higher concentrations (Figure 6). Supplementation with NaCl resulted in moderate increase of activity in a linear correlation (Figure 6) and plateau formation at concentrations between 150 and 200 mM (data not shown).

Figure 6. Influence of buffer composition on the activity of EspP α . Relative activity is normalized to the maximal activity observed for 82.5 mM Mg²⁺. $n = 8$.



Influence of cations on EspI activity is less pronounced compared to EspPa. Activity of EspI is independent of Na^+ (Figure 7a) while the addition of Ca^{2+} and Mg^{2+} resulted in a slight increase in activity. More specific, EspI activity is increased ~ 1.4 -fold by addition of ~ 10 mM of the divalent cations (Figure 7b). Addition of higher concentrations of Ca^{2+} or Mg^{2+} did not further increase activity (Figure 7a).

Figure 7. Influence of buffer composition on the activity of EspI. (a) Relative activity is normalized to the maximal activity observed for 186 mM Mg^{2+} , $n = 4$; (b) Detailed view of cation concentrations in the range from 0 to 9.6 (Na^+) or 9.3 mM (Ca^{2+} , Mg^{2+}).

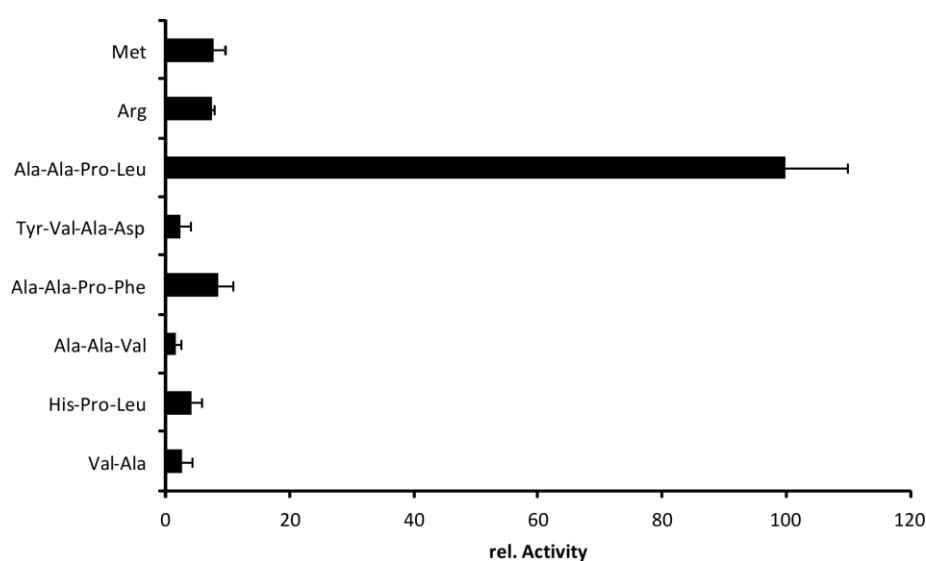


2.5. Cleavage Profile of EspI

Dutta *et al.* (2002) performed a substrate screening with chromogenic peptides for different SPATE members including EspP α [12]. Highest activity of EspP α was observed in this study for Succinic acid-alanine-proline-leucine-(para-nitroaniline) (Suc-Ala-Pro-Leu-pNA) and was confirmed by our group [2,3,12]. However, we did not observe cleavage of H-Arg-Arg-pNA or Bz-Arg-pNA as

described in the initial study (data not shown). To elucidate substrate specificity of EspI, we incubated different chromogenic peptide substrates with EspI and changed substrate recognition sites according to the nomenclature of Schechter and Berger [16] (Figure 8). Like EspP α , EspI efficiently cleaved Suc-Ala-Ala-Pro-Leu-pNA. Modification of substrate sites P1–P4 resulted in significant reduction of relative activity. Hydrophobic amino acids other than leucine at position P1 prevented cleavage nearly completely. Also, exchange of alanine-alanine (P3–P4) to histidine (P3) significantly reduced cleavage of peptide substrates, indicating that EspI exhibits high substrate specificity and an elastase-like substrate profile. High substrate specificity has also been reported for other SPATE members [12,17], and is confirmed for EspI, which belongs to the elastase-like branch of SPATE proteases.

Figure 8. Cleavage profile of EspI. Chromogenic substrates were incubated with EspI. Activity is normalized to the maximal activity observed after incubation of Suc-Ala-Ala-Pro-Leu-pNA, $n = 3$.



3. Experimental Section

3.1. Purification of EspP α and EspI

EspP α was purified from clone HB101 (WB4-5k) containing *espP* from *E. coli* O157:H7 strain EDL933 [1]. The inactive EspP α mutant S263A served as a negative control [2] and EspI was purified in the same way from clone DH5 α /pZH4 containing *espI* from *E. coli* O91:H $^-$ strain 4797/97 [3,6]. Strains were grown overnight in 1 L of LB broth at 37 °C with vigorous shaking. The cultures were centrifuged (6000 \times g, 30 min, 4 °C), supernatants were passed through 0.2 μ m Supor machV bottle-top filters (Nalgene, Rochester, NY, USA), and the supernatant was concentrated 20-fold using Vivaflow 200 PES membrane with 50 kDa molecular weight cut off (Vivascience, Hannover, Germany) and Masterflex easy-load peristaltic pump (Cole Parmer, Vernon Hills, Chicago, IL, USA). Proteins were precipitated (3 h, 4 °C) by adding ammonium sulfate (Merck, Darmstadt, Germany) to 55% saturation. The precipitate was collected by centrifugation (6000 \times g, 30 min, 4 °C) and the pellet was dissolved. For purification of EspP α , the precipitate was dissolved in 10 mM HEPES (*N*-2-hydroxyethylpiperazine-*N'*-2-ethanesulfonic acid) buffer containing 150 mM NaCl (pH 7.4).

EspP α was purified via liquid chromatography (äktä prime FPLC, GE Healthcare, Uppsala, Sweden) using HiTrap Benzamidine FF columns (GE Healthcare, München, Germany) according to the manufacturer's instructions. For purification of EspI, the precipitate was dissolved in 20 mM Tris (tris(hydroxymethyl)aminomethane) buffer containing 50 mM NaCl (pH 6.5). EspI was purified via liquid chromatography using HiPrep 16/10 DEAE FF columns (GE Healthcare, München, Germany) and HiTrap Benzamidine FF columns according to the manufacturer's instructions. Fractions containing EspP α or EspI were collected and concentrated with 10 kDa VivaSpin spin-down filter (Sartorius Stedim Biotech, Göttingen, Germany).

To verify purification of EspP α and EspI, proteases were separated via SDS-PAGE [18,19] and stained with Coomassie blue. Purity was determined (semiquantitatively) by densitometric analysis of Coomassie-stained SDS-PAGE gels using the Chemidoc XRS imager and the Quantity One Software package (both Biorad, Munich, Germany). Proteolytic activity was assessed via incubation of the proteases with chromogenic oligopeptide substrates. 2 μ g of EspP α were incubated in a total volume of 100 μ L HEPES buffer containing 150 mM NaCl and 2 mM succinic acid-alanine-alanine-proline-leucine-(para-nitroaniline) (Suc-Ala-Ala-Pro-Leu-pNA) (Bachem, Weil am Rhein, Germany) (pH 7.4) for 15 h at 37 °C. EspI cleaves the chromogenic oligopeptide substrate considerably faster. Therefore, smaller amounts of EspI were used. Since EspP α was incubated in the buffer used for its purification, the same strategy was applied for EspI. 0.2 μ g of EspI were incubated in a total volume of 100 μ L PBS (phosphate buffered saline, 7.0 mM Na₂HPO₄, 3.0 mM KH₂PO₄) buffer containing 100 mM NaCl and 4.5 mM KCl) and 2 mM Ala-Ala-Pro-Leu-pNA (pH 7.4) for 15 h at 37 °C. The inactive EspP α mutant S263A served as a negative control and was incubated in the same way as EspP α . Activity was analyzed by the photometrical determination of para-nitroaniline release from the chromogenic substrate in a 96-well format using the Dynex Opsis plate reader (Dynex Opsys MR, Berlin, Germany).

3.2. Temperature Optimum of EspP α and EspI

Samples of 2 μ g of EspP α were incubated in a total volume of 100 μ L HEPES buffer containing 150 mM NaCl and 2 mM of the chromogenic oligopeptide substrate Suc-Ala-Ala-Pro-Leu-pNA (pH 7.4) for 12.5 h at temperatures ranging from 16.0 to 54.0 °C. Samples of 0.2 μ g of EspI were incubated in a total volume of 100 μ L PBS buffer containing 100 mM NaCl and 4.5 mM KCl) and 2 mM Ala-Ala-Pro-Leu-pNA (pH 7.4) for 15 h at temperatures ranging from 10.0 to 60.0 °C. To ensure optimal temperature control, the incubation was performed in parallel in a gradient thermocycler (Biometra Gradient Cycler, Göttingen, Germany) at the respective temperatures. The negative control was stored at -20 °C during incubation. Relative activity of EspP α or EspI was analyzed subsequently as the amount of cleaved chromogenic substrate by photometrical determination of released para-nitroaniline at 405 nm in a plate reader using 96-well plates.

3.3. pH Optimum of EspP α and EspI

For the determination of pH optimum, 4 μ g of EspP α were incubated for 15 h at 37 °C in either 166 mM potassium-phthalate buffer (pH 5.4 to 6.4) or in 166 mM Tris buffer (pH 6.0 to 9.1) with 2 mM of the chromogenic substrate Ala-Ala-Pro-Leu-pNA in a total volume of 200 μ L. 0.2 μ g of EspI were

incubated for 15 h at 37 °C in a total volume of 100 µL with 2 mM Suc-Ala-Ala-Pro-Leu-pNA in either 150 mM Tris buffer (pH 5.9 to 8.9) or in 25 mM tetraborate buffer (pH 8.5 to 9.4) because this protease showed activity in a more alkaline environment than EspPα. The pH of the individual buffer stock solutions was adjusted with 2 M HCl or 1 M NaOH, respectively, and re-examined after addition of EspPα or EspI and the chromogenic substrate. The relative activity was analyzed by the photometrical determination of para-nitroaniline release from the chromogenic substrate in a 96-well format using the Dynex Opsis plate reader.

3.4. Effect of Buffer Composition

For incubation of EspPα, stock solutions each containing 100 mM CaCl₂, MgCl₂ or NaCl in 25 mM HEPES, pH 7.4 were diluted with 25 mM HEPES to obtain concentrations of the respective cations ranging from 0 to 82.5 mM. As the HEPES was used as Na-salt, the lowest concentration of Na⁺ was 25 mM in all experiments. In the case of EspI, stock solutions containing 200 mM CaCl₂, MgCl₂ or NaCl in 100 mM Tris, pH 7.4 were diluted with 100 mM Tris leading to concentrations of the respective cations ranging from 0 to 186 mM. As the purified EspI was present in PBS, the lowest concentration of Na⁺ was 0.3 mM in each experiment. These conditions allowed us to investigate a possible effect of even small amounts of Na⁺ on EspI. 2 µg of EspPα or 0.2 µg of EspI were incubated for 15 h at 37 °C with 2 mM of the chromogenic substrate Suc-Ala-Ala-Pro-Leu-pNA in the respective buffer solutions and activity was assessed by photometrical determination of released para-nitroaniline at 405 nm in a Dynex Opsys plate reader.

3.5. Cleavage Profile of EspI

To determine a cleavage profile for EspI, the chromogenic peptides valine-alanine-(para-nitroaniline) (H-Val-Ala-pNA), succinic acid-histidine-proline-leucine-(para-nitroaniline) (Suc-His-Pro-Leu-pNA), succinic acid-alanine-alanine-valine-(para-nitroaniline) (Suc-Ala-Ala-Val-pNA), succinic acid-alanine-alanine-proline-phenylalanine-(para-nitroaniline) (Suc-Ala-Ala-Pro-Phe-pNA), acetyl-tyrosine-valine-alanine-aspartic acid-(para-nitroaniline) (Ac-Tyr-Val-Ala-Asp-pNA), succinic acid-alanine-alanine-proline-leucine-(para-nitroaniline) (Suc-Ala-Ala-Pro-Leu-pNA), benzoyl-arginine-(para-nitroaniline) (Bz-Arg-pNA), and methionine-(para-nitroaniline) (H-Met-pNA) (all Bachem, Weil am Rhein, Germany) were dissolved in dimethylsulfoxide (DMSO). 0.2 µg EspI were incubated for 15 h at 37 °C with 2 mM of chromogenic peptide in 100 µL PBS (pH 7.4) containing 5% DMSO. Activity was assessed by photometrical determination of released para-nitroaniline at 405 nm in a BMG LABTECH FLUOstar Optima plate reader.

4. Conclusions

The analysis of various optima of EspPα regarding temperature, pH, and composition of the solvent suggests that this protease is seemingly well optimized for the conditions at the site of action. EspPα is expressed by EHEC during infection as indicated by the presence of anti-EspPα antibodies in the sera of patients suffering from EHEC [1]. Presumed that EspPα is expressed to act in the human host, the observed temperature optimum is with ~40 °C very close to the situation in the native environment.

This observation is however no matter of course for proteases. As with enzymes in general, the activity of proteases at elevated temperatures is limited mainly by the structural stability of the protein. Rising temperatures lead to increased substrate turnover rates and thus increased enzymatic activity. As a rule, an increase in temperature of 10 °C leads to an approximately twofold elevated enzymatic activity [15]. This principle holds true as long as the native fold of the protease is sustained at the given temperature. As a consequence, proteases with more rigid structures are known, which display temperature optima far beyond their native environmental conditions [20–22]. Based on the data presented in this study, EspP α seems to be “as temperature-stable as necessary” but “as flexible as possible”. This assumption is supported by recent hypotheses concerning the autotransport mechanism of SPATE proteins [23]. During secretion EspP α retains a loosely folded state which is maintained by interaction with several chaperones [24–27]. After translocation through the bacterial outer membrane folding of the proteolytic domain of EspP α is initiated [24]. In addition, Jong *et al.* (2007) have shown that the related SPATE protein Hbp needs a certain degree of flexibility for the efficient translocation through the bacterial cell envelope [28]. Moreover, results of the structure-function analysis of EspP α are in accordance with these findings [2]. It is therefore likely that EspP α is optimized for proteolytic activity at physiological temperatures in the human host but has to retain in addition maximal structural flexibility to fulfill autotransport.

Optimal proteolytic activity of EspP α was observed at slightly alkaline conditions and Ca²⁺ or Mg²⁺ concentrations of approximately 8 mmol/L, suggesting that these conditions mimic best the natural environment of EspP α . Notably, the pH within the human bloodstream is constant between 7.35–7.45 and the concentrations of Ca²⁺ and Mg²⁺ are ~2.5 and ~1 mmol/L and approximately 140 mmol/L Na⁺ [29]. Investigation of the activity of EspP α suggests that Ca²⁺-binding sites within the molecule might contribute to the stability of EspP α . It has been shown for the protease family of subtilases that binding of calcium ions is essential for correct folding and stability [30]. The SPATE protein Hbp/Tsh also exhibits a Ca²⁺-binding domain [31]. Ca²⁺ does not affect the proteolytic activity which lead to the suggestion that it is important for the stability of this protease [31]. Notably, the investigation of potential calcium-binding sites within the crystal structure of EspP α (pdb: 3SZE) [32] using the WebFEATURE program [33] indicated that Ca²⁺ binding might occur at the interfacing α -helical region connecting the proteolytic domain1 and the β -helical backbone as well as in loop 165 (data not shown). Mutagenesis experiments within these regions of EspP α have shown that alterations lead to the loss of proteolytic activity and diminished autotransport, respectively [1,2]. The diminished proteolytic activity of the EspP subtypes β and δ underlies, at least in parts, the modification of the α -helical interface [3]. It is therefore tempting to speculate, that the specific alterations in the proteolytic inactive subtypes β and δ might also affect calcium-binding and thus leads to reduced structural stabilization and consequently to diminished proteolytic activity.

EspI shows, in general, similar biochemical characteristics compared to EspP α . With a temperature optimum of ~38 °C, EspI might also be optimized to act in the human host during STEC infection. Like EspP α , it rapidly loses activity at higher temperatures, demonstrating that this SPATE protease also shows certain flexibility in folding and limited temperature-stability, which might be a necessary feature for autotransport. In direct comparison to EspP α , EspI possibly needs a slightly higher degree of flexibility as demonstrated by the fact that irreversible heat denaturation occurs at lower temperatures. Presuming that the underlying secretion mechanism of EspI is identical as for EspP α [23],

EspI requires a flexible structure during transport across the bacterial outer membrane. Outside of the bacterial outer membrane the flexible passenger domain of EspI might begin to fold, like EspP α , providing a part of the energy necessary for secretion. The EspI precursor, as well as the passenger domain, are slightly larger than the equivalent regions in EspP α and, therefore, might need more temperature sensitive flexible regions to facilitate autotransport. With a pH optimum at slightly alkaline conditions and increased activity at low millimolar concentrations of Ca²⁺ and Mg²⁺, EspI might, like EspP α , be suited to act in the human blood stream. It has however to be noted that the molecular basis of differences in biochemical characteristics between EspP α and EspI still remain elusive as no structure is available for EspI.

Concerning substrate specificity, it is in general believed that differences in specificity amongst SPATE proteins translate into different biological functions including pathogenicity. EspI cleaved Suc-Ala-Ala-Pro-Leu-pNA with high specificity. Exchange of amino acids at position P1 as well as at position P3/P4 strongly reduced cleavage. This high degree of specificity might be associated with specific physiological functions of this protease, which need to be elucidated in future studies.

Acknowledgments

This study was supported by the Deutsche Forschungsgemeinschaft (DFG) grant BR 4258/1-1.

Author Contributions

A.W. designed and conducted experiments, discussed results, and prepared the manuscript; D.K. designed and conducted experiments and discussed manuscript preparation; J.B. designed and conducted experiments, discussed results, prepared the manuscript and secured funding of the study.

Conflicts of Interest

The authors declare no conflict of interest.

References

1. Brunder, W.; Schmidt, H.; Karch, H. EspP, a novel extracellular serine protease of enterohaemorrhagic *Escherichia coli* O157:H7 cleaves human coagulation factor V. *Mol. Microbiol.* **1997**, *24*, 767–778.
2. Brockmeyer, J.; Spelten, S.; Kuczius, T.; Bielaszewska, M.; Karch, H. Structure and function relationship of the autotransport and proteolytic activity of EspP from Shiga toxin-producing *Escherichia coli*. *PLoS One* **2009**, *4*, e6100.
3. Brockmeyer, J.; Bielaszewska, M.; Fruth, A.; Bonn, M.L.; Mellmann, A.; Humpf, H.U.; Karch, H. Subtypes of the plasmid-encoded serine protease EspP in Shiga toxin-producing *Escherichia coli*: Distribution, secretion, and proteolytic activity. *Appl. Environ. Microbiol.* **2007**, *73*, 6351–6359.
4. Bielaszewska, M.; Stoewe, F.; Fruth, A.; Zhang, W.; Prager, R.; Brockmeyer, J.; Mellmann, A.; Karch, H.; Friedrich, A.W. Shiga toxin, cytolethal distending toxin, and hemolysin repertoires in clinical *Escherichia coli* O91 isolates. *J. Clin. Microbiol.* **2009**, *47*, 2061–2066.

5. Khan, A.B.; Naim, A.; Orth, D.; Grif, K.; Mohsin, M.; Prager, R.; Dierich, M.P.; Wurzner, R. Serine protease espP subtype alpha, but not beta or gamma, of Shiga toxin-producing *Escherichia coli* is associated with highly pathogenic serogroups. *Int. J. Med. Microbiol.* **2009**, *299*, 247–254.
6. Schmidt, H.; Zhang, W.L.; Hemmrich, U.; Jelacic, S.; Brunder, W.; Tarr, P.I.; Dobrindt, U.; Hacker, J.; Karch, H. Identification and characterization of a novel genomic island integrated at selC in locus of enterocyte effacement-negative, Shiga toxin-producing *Escherichia coli*. *Infect. Immun.* **2001**, *69*, 6863–6873.
7. Orth, D.; Ehrlenbach, S.; Brockmeyer, J.; Khan, A.B.; Huber, G.; Karch, H.; Sarg, B.; Lindner, H.; Wurzner, R. EspP, a serine protease of enterohemorrhagic *Escherichia coli*, impairs complement activation by cleaving complement factors C3/C3b and C5. *Infect. Immun.* **2010**, *78*, 4294–4301.
8. Brockmeyer, J.; Aldick, T.; Soltwisch, J.; Zhang, W.; Tarr, P.I.; Weiss, A.; Dreisewerd, K.; Muthing, J.; Bielaszewska, M.; Karch, H.; et al. Enterohaemorrhagic *Escherichia coli* haemolysin is cleaved and inactivated by serine protease EspPalpha. *Environ. Microbiol.* **2011**, *13*, 1327–1341.
9. Dos Santos, L.F.; Irino, K.; Vaz, T.M.; Guth, B.E. Set of virulence genes and genetic relatedness of O113:H21 *Escherichia coli* strains isolated from the animal reservoir and human infections in Brazil. *J. Med. Microbiol.* **2010**, *59*, 634–640.
10. Toszeghy, M.; Phillips, N.; Reeves, H.; Wu, G.; Teale, C.; Coldham, N.; Randall, L. Molecular and phenotypic characterisation of Extended Spectrum beta-lactamase CTX-M *Escherichia coli* from farm animals in Great Britain. *Res. Vet. Sci.* **2012**, *93*, 1142–1150.
11. Abreu, A.G.; Bueris, V.; Porangaba, T.M.; Sircili, M.P.; Navarro-Garcia, F.; Elias, W.P. Autotransporter protein-encoding genes of diarrheagenic *Escherichia coli* are found in both typical and atypical enteropathogenic *E. coli*. *Appl. Environ. Microbiol.* **2012**, doi:10.1128/AEM.02635-12.
12. Dutta, P.R.; Cappello, R.; Navarro-Garcia, F.; Nataro, J.P. Functional Comparison of Serine Protease Autotransporters of Enterobacteriaceae. *Infect. Immun.* **2002**, *70*, 7105–7113.
13. Puttamreddy, S.; Cornick, N.A.; Minion, F.C. Genome-wide transposon mutagenesis reveals a role for pO157 genes in biofilm development in *Escherichia coli* O157:H7 EDL933. *Infect. Immun.* **2010**, *78*, 2377–2384.
14. Xicohtencatl-Cortes, J.; Saldana, Z.; Deng, W.; Castaneda, E.; Freer, E.; Tarr, P.I.; Finlay, B.B.; Puente, J.L.; Giron, J.A. Bacterial macroscopic rope-like fibers with cytopathic and adhesive properties. *J. Biol. Chem.* **2010**, *285*, 32336–32342.
15. Christen, P.; Jaussi, R. *Biochemie*, 1st ed.; Springer: Berlin/Heidelberg, Germany, 2005; Volume 1.
16. Schechter, I.; Berger, A. On the size of the active site in proteases. I. Papain. *Biochem. Biophys. Res. Commun.* **1967**, *27*, 157–162.
17. Dautin, N. Serine Protease Autotransporters of Enterobacteriaceae (SPATEs): Biogenesis and Function. *Toxins* **2010**, *2*, 1179–1206.
18. Laemmli, U.K. Cleavage of structural proteins during the assembly of the head of bacteriophage T4. *Nature* **1970**, *227*, 680–685.
19. Schagger, H.; von Jagow, G. Tricine-sodium dodecyl sulfate-polyacrylamide gel electrophoresis for the separation of proteins in the range from 1 to 100 kDa. *Anal. Biochem.* **1987**, *166*, 368–379.

20. Helland, R.; Larsen, A.N.; Smalas, A.O.; Willassen, N.P. The 1.8 Å crystal structure of a proteinase K-like enzyme from a psychrotroph *Serratia* species. *FEBS J.* **2006**, *273*, 61–71.
21. Huesgen, P.F.; Scholz, P.; Adamska, I. The serine protease HhoA from *Synechocystis* sp. strain PCC 6803: Substrate specificity and formation of a hexameric complex are regulated by the PDZ domain. *J. Bacteriol.* **2007**, *189*, 6611–6618.
22. Patel, A.K.; Singh, V.K.; Jagannadham, M.V. Carnein, a serine protease from noxious plant weed *Ipomoea carnea* (morning glory). *J. Agric. Food Chem.* **2007**, *55*, 5809–5818.
23. Weiss, A.; Brockmeyer, J. Prevalence, biogenesis, and functionality of the serine protease autotransporter EspP. *Toxins* **2013**, *5*, 25–48.
24. Ieva, R.; Bernstein, H.D. Interaction of an autotransporter passenger domain with BamA during its translocation across the bacterial outer membrane. *Proc. Natl. Acad. Sci. USA* **2009**, *106*, 19120–19125.
25. Ruiz-Perez, F.; Henderson, I.R.; Leyton, D.L.; Rossiter, A.E.; Zhang, Y.; Nataro, J.P. Roles of periplasmic chaperone proteins in the biogenesis of serine protease autotransporters of Enterobacteriaceae. *J. Bacteriol.* **2009**, *191*, 6571–6583.
26. Ruiz-Perez, F.; Henderson, I.R.; Nataro, J.P. Interaction of FkpA, a peptidyl-prolyl *cis/trans* isomerase with EspP autotransporter protein. *Gut Microbes* **2010**, *1*, 339–344.
27. Ieva, R.; Skillman, K.M.; Bernstein, H.D. Incorporation of a polypeptide segment into the beta-domain pore during the assembly of a bacterial autotransporter. *Mol. Microbiol.* **2008**, *67*, 188–201.
28. Jong, W.S.; ten Hagen-Jongman, C.M.; den Blaauwen, T.; Slotboom, D.J.; Tame, J.R.; Wickstrom, D.; de Gier, J.W.; Otto, B.R.; Luirink, J. Limited tolerance towards folded elements during secretion of the autotransporter Hbp. *Mol. Microbiol.* **2007**, *63*, 1524–1536.
29. Jelkmann, W. Blut und Immunabwehr. In *Physiologie des Menschen*, 30 bearbeitete und aktualisierte Auflage ed.; Springer: Berlin/Heidelberg, Germany, 2007; Volume 30, pp. 523–549.
30. Siezen, R.J.; Leunissen, J.A. Subtilases: The superfamily of subtilisin-like serine proteases. *Protein Sci.* **1997**, *6*, 501–523.
31. Nishimura, K.; Yoon, Y.H.; Kurihara, A.; Unzai, S.; Luirink, J.; Park, S.Y.; Tame, J.R. Role of domains within the autotransporter Hbp/Tsh. *Acta Crystallogr. D* **2010**, *66*, 1295–1300.
32. Khan, S.; Mian, H.S.; Sandercock, L.E.; Chirgadze, N.Y.; Pai, E.F. Crystal structure of the passenger domain of the *Escherichia coli* autotransporter EspP. *J. Mol. Biol.* **2011**, *413*, 985–1000.
33. Liang, M.P. WebFEATURE: An interactive web tool for identifying and visualizing functional sites on macromolecular structures. *Nucleic Acids Res.* **2003**, *31*, 3324–3327.